Synthesis, Characterization, and Thermal Degradation Kinetics of the Copolymer Poly(4-methoxybenzyl methacrylate-*co*-isobornyl methacrylate)

Adnan Kurt,[1] Esin Kaya[2]

[1]*Department of Chemistry, Faculty of Arts and Sciences, University of Adiyaman, 02040, Adiyaman, Turkey*
[2]*Department of Science Education, Faculty of Education, University of Mus Alparslan, 49100 Mus, Turkey*

Received 5 March 2009; accepted 15 July 2009
DOI 10.1002/app.31162
Published online 14 October 2009 in Wiley InterScience (www.interscience.wiley.com).

ABSTRACT: A copolymer of 4-methoxybenzyl methacrylate and isobornyl methacrylate was synthesized by atom transfer radical polymerization. The structure of poly(4-methoxybenzyl methacrylate-*co*-isobornyl methacrylate) was confirmed by means of Fourier transform infrared, ^{1}H-NMR, and ^{13}C-NMR techniques. The molecular weight distribution values of the copolymer were determined with gel permeation chromatography. The number-average molecular weight and polydispersity index values of poly(4-methoxybenzyl methacrylate-*co*-isobornyl methacrylate) were found to be 12,500 and 1.5, respectively. The kinetics of the thermal degradation of the copolymer was investigated with thermogravimetric analysis at different heating rates. The activation energy values obtained with the Kissinger, Flynn–Wall–Ozawa, and Tang methods were determined to be 166.38, 167.54, and 167.47 kJ/mol, respectively. Different integral and differential methods were used, and the results were compared with these values. Doyle approximation was also used for comparing the experimental results to master plots. An analysis of the experimental results suggested that the reaction mechanism was an R_1 deceleration type in the conversion range studied. © 2009 Wiley Periodicals, Inc. J Appl Polym Sci 115: 2359–2367, 2010

Key words: activation energy; atom transfer radical polymerization (ATRP); copolymerization; thermogravimetric analysis (TGA)

INTRODUCTION

Recently, controlled living radical polymerizations have been used for the synthesis of well-defined, narrow-dispersity polymers.[1,2] One of the most successful methods is atom transfer radical polymerization (ATRP) based on a copper halide and a nitrogen catalyst.[3,4] Because ATRP is a controlled/living radical polymerization, well-defined polymers, with molecular weights determined by the ratio of the consumed monomer to the introduced initiator, are obtained:

$$\Delta P_n = \Delta[\mathrm{M}]/[\mathrm{I}_0]$$

where ΔP_n is the degree of polymerization, [M] is the monomer concentration and $[\mathrm{I}_0]$ is the initial initiator concentration. Polydispersities are generally low and change as follows: $1.0 < M_w/M_n < 1.5$ (where M_w is the weight-average molecular weight and M_n is the number-average molecular weight).[5] Because of its mechanism, ATRP allows the preparation of more precisely controlled polymer, and many new materials have been synthesized.[6,7] This process generates oxidized metal complexes as persistent radicals to reduce the stationary concentration of growing radicals and thereby minimize the contribution of termination. Successful ATRP will have not only a small contribution of terminated chains but also uniform growth of all chains, and this is an accomplished through fast initiation and rapid reversible deactivation.[5] Kinetic considerations indicate that the composition of statistical copolymers prepared by ATRP should be identical to that of copolymers prepared under conventional radical polymerization conditions.[8]

(Meth)acrylic copolymers have achieved prime importance in various avenues of industrial applications.[9–11] For example, copolymers formed from substituted phenyl methacrylate are used in the production of printing plates and electrical circuits.[12,13] Moreover, copolymerization is an important and useful way to develop new materials. Copolymerization modulates both the intramolecular and intermolecular forces exercised between polymer segments. Therefore, some properties, such as the procedural decomposition temperatures (initial and final) with respect to thermal degradation and the glass-transition temperature, may vary within wide limits.[14]

Correspondence to: A. Kurt (adnkurt@gmail.com).

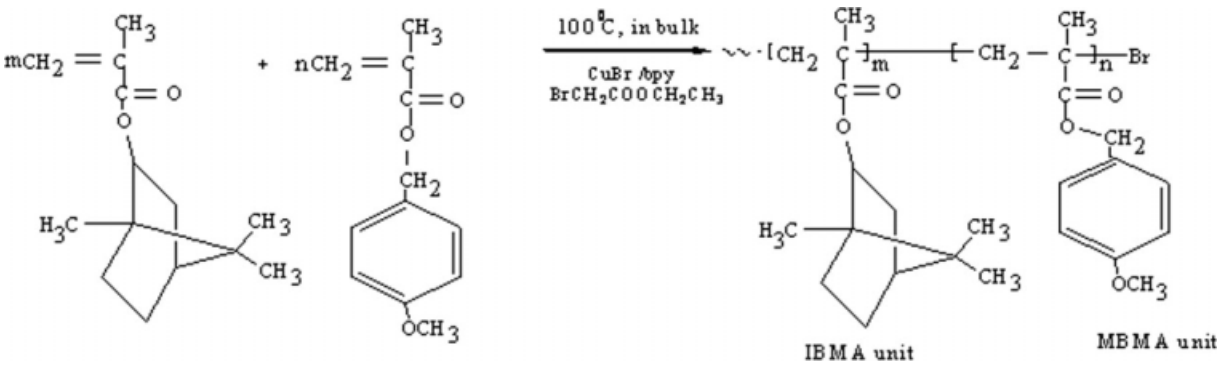

Scheme 1 Synthesis of poly(MBMA-*co*-IBMA).

Thermal degradation studies of polymers are necessary as many applications depend on their thermal stability. To accomplish this goal, thermogravimetric analysis is a technique widely used because of its simplicity and the information afforded by a simple thermogram.[15] The thermal degradation expression results change according to different assumptions and derivatives; for example, the state (bulk or powder), carrier gas, and flow rate directly affect the parameter results.[16] Many of the methods of kinetic analysis are based on the hypothesis that, from a simple thermogravimetric trace, meaningful values can be obtained for parameters such as the activation energy, pre-exponential factor, and reaction order. Many studies designed to evaluate experimental data have employed reference theoretical curves, which are often known as master plots.[17–20] In this sense, the master plot can be considered a characteristic curve that is independent of the measurement conditions and is easily obtained from experimental data.

This article reports the synthesis, characterization, and thermal degradation kinetics of the copolymer poly(4-methoxybenzyl methacrylate-*co*-isobornyl methacrylate) [poly(MBMA-*co*-IBMA)].

EXPERIMENTAL

Materials

All chemicals and solvents used in this study were analytical-grade. The main chemicals used in this study were as follows. 4-Methoxybenzylbromide (analytical reagent), sodium methacrylate, cuprous(I) bromide, 2,2′-bipyridine (bpy), and ethyl 2-bromoacetate (analytical reagent) were used as received. Isobornyl methacrylate (IBMA) was vacuum-distilled after being washed with a 5% NaOH aqueous solution just before copolymerization.

Synthesis of 4-methoxybenzyl methacrylate (MBMA)

MBMA was synthesized by the reaction of 4-methoxybenzylbromide and sodium methacrylate at 0–5°C with potassium carbonate and tetrahydrofuran (THF). It was distilled *in vacuo* (bp = 114°C at 20 mmHg). The monomer was characterized with FTIR, ^{1}H-NMR, and ^{13}C-NMR techniques.

^{1}H-NMR ($CDCl_3$, δ, ppm): 7.24–6.89 (4H, aromatic ring protons), 6.01 and 5.52 (2H, CH_2=C), 5.01 (2H, —OCH_2—), 3.74 (3H, CH_3O—Ar), 1.93 (3H, α-methyl). FTIR (cm^{-1}, the most characteristic bands): 1715 (C=O stretching), 1638 (C=C stretching in the vinyl group), 1611 (C=C stretching in the aromatic ring). ^{13}C-NMR ($CDCl_3$, δ, ppm): 166.86 (C=O), 159.59 (ipso carbon on the aromatic ring), 136.18 (=C), 124.9–128.2 (=CH on the aromatic ring), 66.05 (—OCH_2—), 55.0 (—OCH_3), 18.0 (—CH_3).

ATRP copolymerization of MBMA with IBMA

The general procedure for the copolymerization of MBMA with IBMA was as follows. Predetermined amounts of the monomers, initiator (ethyl 2-bromoacetate), ligand (bpy), and CuBr as a catalyst were added to a flask. The mixture was degassed three times by freeze–pump–thaw cycles and sealed *in vacuo*. The flask was shaken until the mixture dissolved, was immersed in an oil bath, and was heated to the required temperature (100°C). After a particular amount of time, the flask was opened, and dichloromethane was added to the sample to dissolve the copolymer. The heterogeneous solution was filtered. The copolymer was isolated by precipitation in *n*-hexane and dried at 40°C for 24 h (Scheme 1). The conversion of the copolymerization was determined gravimetrically. The ^{1}H-NMR and FTIR data for poly(MBMA-*co*-IBMA) were as follows.

^{1}H-NMR ($CDCl_3$, δ, ppm): 7.25–6.87 (4H, aromatic ring protons of MBMA units), 4.97 (2H, —OCH_2 protons of MBMA units; 1H, —OCH— protons of IBMA units), 3.75 (3H, CH_3O—Ar), 1.98–0.67 (—CH—, —CH_2—, and —CH_3 protons in main-chain and side groups). FTIR (cm^{-1}, the most characteristic bands): 3037–2836 (aromatic and aliphatic C—H stretching), 1780 (C=O stretching in the lactone ring), 1724 (C=O stretching), 1638 (C=C stretching in the vinyl group), 1613 (C=C stretching in the aromatic ring).

TABLE I
Algebraic Expressions for $g(\alpha)$ for the Most Frequently Used Mechanisms of the Solid-State Processes

Symbol	$g(\alpha)$	Solid-state process
Sigmoidal curves		
A_2	$[-\ln(1-\alpha)]^{1/2}$	Nucleation and growth [Avrami eq. (1)]
A_3	$[-\ln(1-\alpha)]^{1/3}$	Nucleation and growth [Avrami eq. (2)]
A_4	$[-\ln(1-\alpha)]^{1/4}$	Nucleation and growth [Avrami eq. (3)]
Deceleration curves		
R_1	α	Phase-boundary-controlled reaction (one-dimensional movement)
R_2	$[1-(1-\alpha)^{1/2}]$	Phase-boundary-controlled reaction (contraction area)
R_3	$[1-(1-\alpha)^{1/3}]$	Phase-boundary-controlled reaction (contraction volume)
D_1	α^2	One-dimensional diffusion
D_2	$(1-\alpha)\ln(1-\alpha)+\alpha$	Two-dimensional diffusion
D_3	$[1-(1-\alpha)^{1/3}]^2$	Three-dimensional diffusion (Jander equation)
D_4	$(1-2/3\alpha)(1-\alpha)^{2/3}$	Three-dimensional diffusion (Ginstling–Brounshtein equation)
F_2	$1/(1-\alpha)$	Random nucleation with two nuclei on the individual particle
F_3	$1/(1-\alpha)^2$	Random nucleation with three nuclei on the individual particle

Instrumental techniques

Infrared spectra were recorded on a PerkinElmer Spectrum One and obtained with a polymeric film on a salt plate. ^{1}H-NMR spectra were recorded on a JEOL FX 90Q NMR spectrometer at room temperature with $CDCI_3$ as a solvent and tetramethylsilane as an internal standard. Gel permeation chromatography analyses were carried out with a high-pressure liquid chromatography pump with an Agilent 1100 system equipped with a vacuum degasser and a refractive-index detector. The eluting solvent was THF, and the flow rate was 1 mL/min. The calibration was achieved with polystyrene standards. Differential scanning calorimetry (DSC) measurements were carried out with a Shimadzu DSC-50 analyzer under a nitrogen flow at a heating rate of 20°C/min. Thermogravimetric analysis was performed with a Shimadzu TGA-50 analyzer. The thermal stability and decomposition activation energy measurements were carried out from the ambient temperature to 500°C at heating rates of 5, 15, 25, and 35°C/min. All the experiments were carried out under a nitrogen atmosphere. The optimum gas flow rate was used 25 mL/min for the TGA-50 analyzer. For thermogravimetric analysis, the polymer samples were evaluated in the form of 4–8-mg weights.

Thermal decomposition kinetics

The application of dynamic thermogravimetry methods holds great promise as a tool for unraveling the mechanisms of physical and chemical processes that occur during polymer degradation. The rate of solid-state isothermal decomposition reactions can be expressed as follows:

$$\frac{d\alpha}{dT}=\frac{A}{\beta}e^{-\frac{E}{RT}}f(\alpha) \tag{1}$$

where α is the degree of conversion, T is the absolute temperature (K), A is the pre-exponential factor (min^{-1}), E is the activation energy (kJ/mol), R is the gas constant (8.314 J mol^{-1} K^{-1}) and, $f(\alpha)$ is a function depending on the reaction mechanism. The rearrangement of eq. (1) and the integration of both sides of the equation lead to the following expression

$$g(\alpha)=\int_0^{\alpha_p}\frac{d\alpha}{f(\alpha)}=\frac{A}{\beta}\int_0^{T_p}e^{-\frac{E}{RT}}dT \tag{2}$$

where $g(\alpha)$ is the integral function of conversion. In the case of polymers, the degradation process follows either a sigmoidal function or a deceleration function and T_p corresponds to peak temperature and α_p is degree of conversion at peak temperature. Table I shows different expressions of $g(\alpha)$ for the different solid-state mechanisms.[21–23]

Kissinger method[24]

The activation energy can be determined by the Kissinger method without a precise knowledge of the reaction mechanism with the following equation:

$$\ln\left(\frac{\beta}{{T_{max}}^2}\right)=\left\{\ln\frac{AR}{E}+\ln\left[n(1-\alpha_{max})^{n-1}\right]\right\}-\frac{E}{RT_{max}} \tag{3}$$

where β is the heating rate, T_{max} is the temperature corresponding to the inflection point of the thermodegradation curve that corresponds to the maximum reaction rate, α_{max} is the maximum conversion, and n is the reaction order. From a plot of $\ln(\beta/T_{max}^2)$ versus $1000/T_{max}$ with fitting to a straight line, the activation energy can be calculated from the slope.

Flynn–Wall–Ozawa method[25,26]

This method was derived from the integral method, which can determine the activation energy without knowledge of the reaction order. It is used to determine the activation energy for given conversion values. With the Doyle approximation,[27] eq. (2) may then be integrated to give the following in logarithmic form:

$$\log \beta = \log\left[\frac{AE}{g(\alpha)R}\right] - 2.315 - \frac{0.457E}{RT} \tag{4}$$

The activation energy for different conversion values can be calculated from a plot of ln β versus $1000/T$.

Tang method[28]

With the logarithms of the side taken and with an approximation formula used for the solution of eq. (2), the following equation can be obtained:

$$\ln\left(\frac{\beta}{T^{1.894661}}\right) = \ln\left[\frac{AE}{Rg(\alpha)}\right] + 3.635041 - 1.894661 \ln E - \frac{1.001450E}{RT} \tag{5}$$

Plots of $\ln(\beta/T^{1.894661})$ versus $1/T$ yield a group of straight lines. The activation energy can be obtained from the slope of $-1.001450E/R$ of the regression line.

Coats–Redfern method[29]

The Coats–Redfern method uses an asymptotic approximation for the resolution of eq. (2):

$$\ln\frac{g(\alpha)}{T^2} = \ln\frac{AR}{\beta E} - \frac{E}{RT} \tag{6}$$

The activation energy for every degradation process listed in Table I can be determined from a plot of ln $g(\alpha)$ versus $1000/T$.

Van Krevelen method[30] and Horowitz–Metzger method[31]

Van Krevelen et al.[30] conducted the first serious theoretical treatment of thermogravimetric data. These authors approximated the exponential integral to obtain a final equation in logarithmic form:

$$\log g(\alpha) = \log B + \left(\frac{E}{RT_r} + 1\right)\log T \tag{7}$$

where

$$B = \frac{A}{\beta}\left(\frac{E}{RT_r} + 1\right)^{-1}\left(\frac{0.368}{T_r}\right)^{\frac{E}{RT_r}}$$

and T_r is the reference temperature. Horowitz and Metzger[31] simplified the exponential integral, using an approximation similar to Van Krevelen et al. and defining a characteristic temperature (θ) such that $\theta = T - T_r$. Making the approximation

$$\frac{1}{T} = \frac{1}{T_r + \theta} \cong \frac{1}{T_r} - \frac{\theta}{T_r^2}$$

they finally obtained for $n = 1$

$$\ln g(\alpha) = \frac{E\theta}{RT_r^2} \tag{8}$$

In this study, to obtain reproducible results, T_r was taken as the temperature corresponding to the maximum temperature rate. With either of these methods, the activation energy can be determined without the precise knowledge of the thermodegradation kinetics.

Criado method for the determination of the reaction mechanism[22]

The activation energy of a solid-state reaction can be determined from several nonisothermal measurements, whatever the reaction mechanism is. If the value of the activation energy is known, the kinetic model of the process can be found in the following way. Criado et al.[22] defined the following function:

$$z(\alpha) = \frac{\left(\frac{d\alpha}{dt}\right)}{\beta}\pi(x)T \tag{9}$$

where $x = E/RT$ and $\pi(x)$ is an approximation of the temperature integral, which cannot be expressed in a simple analytical form. In this study, the fourth rational expression proposed by Senum and Yang[32] was used:

$$z(\alpha) = f(\alpha)g(\alpha) \tag{10}$$

This equation was used to obtain the master curves as a function of the reaction degree corresponding to the different models listed in Table I.

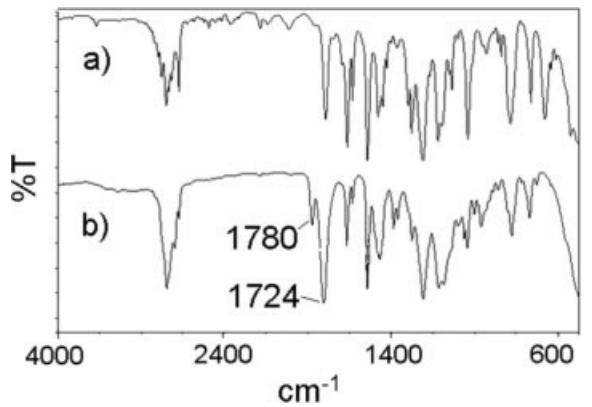

Figure 1 IR spectra of (a) MBMA and (b) poly(MBMA-*co*-IBMA).

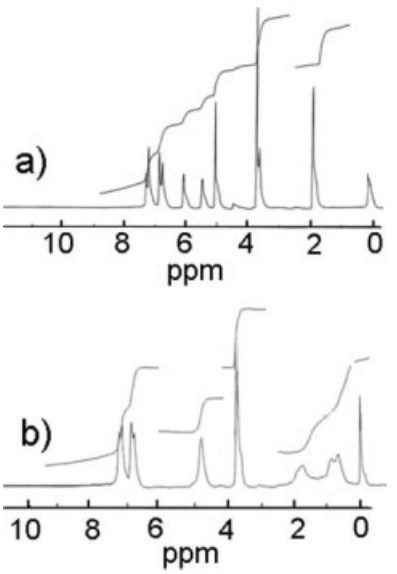

Figure 2 ^{1}H-NMR spectra of (a) MBMA and (b) poly (MBMA-*co*-IBMA).

RESULTS AND DISCUSSION

The copolymer of MBMA and IBMA was synthesized by the ATRP method with ethyl 2-bromoacetate as the initiator and CuBr/bpy as the catalytic system. The molar ratio of the compounds in the ATRP system was 1 : 1 : 2 : 100 [initiator/Cu(I)Br/bpy/monomers]. The copolymer composition was calculated with the aid of integration heights at 6.87–7.25 (4H, aromatic protons of MBMA units) and 4.97 ppm (2H, —OCH_2— protons of MBMA; 1H, —OCH— protons of IBMA). Thus, the percentages of MBMA and IBMA units in the copolymer composition were determined to be 76 and 24%, respectively. The FTIR and ^{1}H-NMR spectra of the MBMA monomer and poly(MBMA-*co*-IBMA) copolymer are presented in Figures 1(a,b) and 2(a,b), respectively. In particular, the small band at 1780 cm^{-1} shown in Figure 1(b) is characteristic of the carbonyl group in a lactone ring with five members. It may be suggested that a lactone ring forms with the removal of benzyl bromide at the chain end if MBMA units exist at the copolymer chain end during copolymerization when the ATRP temperature is 110°C, as shown in Scheme 2. This band was not observed for the poly(benzyl methacrylate) homopolymer; its structure was similar to that of MBMA when it was synthesized under free-radical polymerization conditions in a study reported by Demirelli et al.[7] The MBMA monomer was also characterized with the ^{13}C-NMR technique. The ^{13}C-NMR spectrum of MBMA is shown in Figure 3. The M_n and molecular weight distribution values of poly(MBMA-*co*-IBMA) were found to be 12,500 and 1.5, respectively. From these results, it can be said that the copolymerization was controlled/living.[5,6] Also, they suggest that the contribution of chain breaking and transfer as well as termination reactions during polymerization can be neglected.[5] The glass-transition temperatures of the homopolymers and copolymer were determined by DSC. The DSC curves of the polymers are shown in Figure 4. The glass-transition temperatures of the homopolymers poly(4-methoxybenzyl methacrylate) [poly(MBMA)] and poly(isobornyl methacrylate) [poly(IBMA)] were determined to be 55 and 198°C, respectively. The prepared copolymer showed a single glass-transition temperature at 76°C, which demonstrated the absence of the formation of a mixture

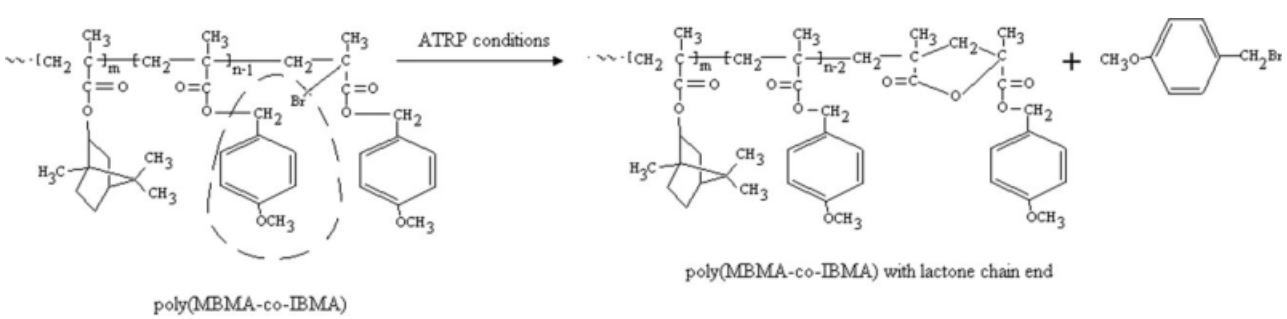

Scheme 2 Poly(MBMA-*co*-IBMA) with a lactone chain end.

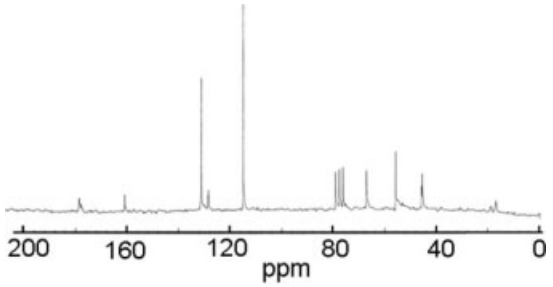

Figure 3 ^{13}C-NMR spectrum of MBMA.

of the homopolymers or the formation of a block copolymer. From these results, it was observed that there was no phase separation between MBMA and IBMA units in the copolymer chains.

Thermal decomposition curves of the poly (MBMA-*co*-IBMA) copolymer carried out at different heating rates of 5, 15, 25, and 35°C/min are shown in Figure 5. After complete degradation, the initial decomposition temperature, decomposition temperature at 50% weight loss, weight loss (%) at 300 and 350°C, and residual mass at 500°C were determined from these curves, and they are presented in Table II. From the corresponding dynamic thermogravimetry profiles, the temperatures related to the maximum decomposition rates for heating rates of 5, 15, 25, 35, and 45°C/min were found to be 288.3, 304.23, 315.5, 316.8, and 322.8°C, respectively. An analysis of these curves shows that, at 500°C, the residue decreased 9.8% with a 15°C/min heating rate. The 10°C/min intervals between measurements were chosen to avoid the overlapping of inflection point temperatures.[23]

According to the Kissinger method, the activation energy can be calculated from a plot of $\ln(\beta/T_{max}^2)$ versus $1000/T_{max}$ and with fitting to a straight line with eq. (3). According to Figure 6, the activation energy obtained with this method was 166.38 kJ/mol. The activation energy can also be determined with the Flynn–Wall–Ozawa method [eq. (4)] from a linear fitting of log β versus $1000/T$ at different conversions. Because this equation was derived with the Doyle approximation, only conversion values in the range of 5–20% can be used. For this study, we used the conversion values of 3, 5, 7, 9, 12, 15, and 18%. Figure 7 shows that the fitting straight lines are nearly parallel, thus indicating the applicability of this method to our copolymer in the conversion range studied. Table III shows the activation energies corresponding to the different conversions calculated with the Flynn–Wall–Ozawa method. A mean value of 167.54 kJ/mol was found from these values. Table III also shows that the activation energy corresponding to 18% conversion (167.26 kJ/mol) was very close to the value obtained with the Kissinger method (166.38 kJ/mol).

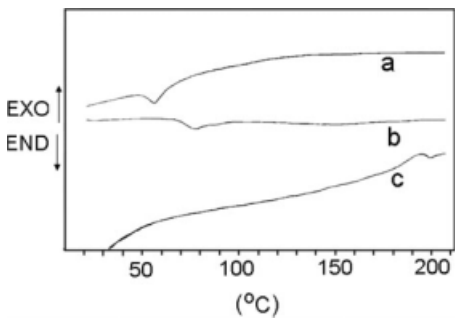

Figure 4 DSC curves of (a) poly(MBMA), (b) poly (MBMA-*co*-IBMA), and (c) poly(IBMA).

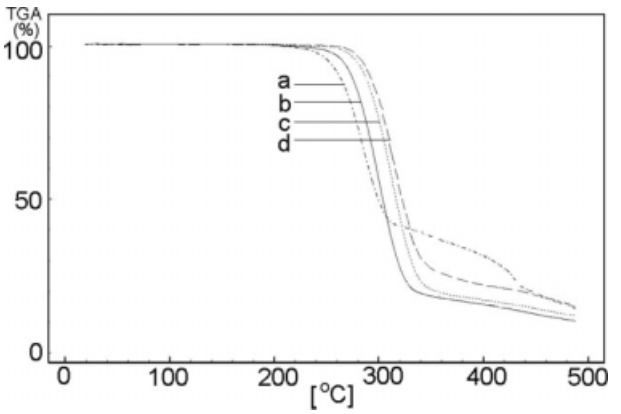

Figure 5 Experimental thermogravimetric analysis (TGA) curves at different heating rates: (a) 5, (b) 15, (c) 25, and (d) 35°C/min.

For the determination of the activation energy, another isoconversion method used in this study was the Tang method. According to this method [using eq. (5)], the activation energy can be calculated from a plot of $\ln(\beta/T^{1.894661})$ versus $1000/T$ fit to a straight line. Figure 8 shows the fitting straight lines determined by the Tang method applied to the experimental data at various conversion values in the range of 3–18%. The calculated results are summarized in Table III. The mean value of the

TABLE II
Thermogravimetric Analysis Data at Different Heating Rates

Reaction rate (°C/min)	T_i[a]	$T_{50\%}$ (°C)[b]	Weight loss at 300°C (%)	Weight loss at 350°C (%)	Residue at 500°C (%)
5	227.9	300.0	50	62	13.9
15	239.1	304.4	44	82	9.8
25	250.3	318.2	23	79	12.5
35	255.4	322.2	17	73	14.9

[a] Initial decomposition temperature (°C).
[b] Temperature at 50% decomposition.

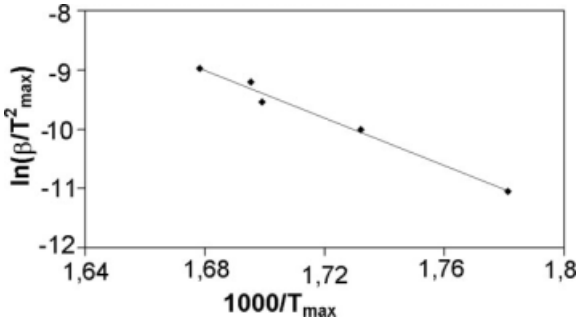

Figure 6 Kissinger method applied to the experimental data at different heating rates.

TABLE III
Activation Energy (E_a) Values Obtained with the Flynn–Wall–Ozawa and Tang Methods

	Flynn–Wall–Ozawa method		Tang method	
α (%)	E_a (kJ/mol)	R	E_a (kJ/mol)	R
3	159.07	0.9977	158.82	0.9974
5	168.79	0.9900	168.91	0.9890
7	162.65	0.9806	162.37	0.9785
9	171.37	0.9865	171.48	0.9851
12	173.83	0.9772	173.99	0.9748
15	169.84	0.9554	169.74	0.9508
18	167.26	0.9635	166.96	0.9596
Mean	167.54		167.47	

activation energy (167.47 kJ/mol) was very close to the value obtained with the Kissinger method (166.38 kJ/mol) and the Flynn–Wall–Ozawa method (167.54 kJ/mol). Compared to other methods, these three methods have the advantage that they do not require previous knowledge of the reaction mechanism for determining the activation energy. To check thermodegradation mechanism models, these methods have been used by some authors.[23,33]

The activation energy for every $g(\alpha)$ function listed in Table I was proposed by Coats and Redfern[29] using eq. (6). These values were obtained at constant heating rates from the fitting of $\ln[g(\alpha)/T^2]$–$1000/T$ plots. In this study, we used the same conversion values. Tables IV and V show activation energies and correlations for conversions in the range of 3–18% at constant heating rates of 5, 15, 25, and 35°C/min. An analysis of these tables shows that, at all the heating rates, the activation energies in better agreement with those obtained with the Kissinger method corresponded to an R_n-type mechanism. For comparison, we chose the Kissinger and Flynn–Wall–Ozawa methods because they are independent of a particular kinetic mechanism. Also, from these tables, it can be seen that the optimum heating rates were 15 and 35°C/min, at which the activation energy corresponding to an R_1 mechanism at a heating rate of 15°C/min was 171.67 kJ/mol, which was very close to the values obtained with the Flynn–Wall–Ozawa method (167.54 kJ/mol) and the Kissinger method (166.38 kJ/mol). These facts strongly suggest that the solid-state thermodegradation mechanism followed by the poly(MBMA-*co*-IBMA) copolymer is a deceleration type (R_n). However, an R_1 mechanism needs less energy to start. The R_2 and R_3 mechanisms are also possible; the activation energy values of R_2 and R_3 mechanisms for 15°C/min are 175.72 and 177.10 kJ/mol, respectively.

We calculated activation energies and correlations with the Van Krevelen[30] and Horowitz and Metzger[31] models to confirm this behavior. The activation energies were obtained through a linear fitting of log $g(\alpha)$–log T plots with eq. (7). Table VI shows the activation energies and correlation values for R_n mechanisms at different constant heating rates. According to this table, mechanism R_1, at a heating rate of 35°C/min, yielded results in better agreement with those obtained with the Flynn–Wall–Ozawa method (167.54 kJ/mol). At the same time, the best correlation (0.9977) was that corresponding to 35°C/min, and this was in good agreement with the value obtained with the Coats–Redfern method (0.9974). Table VII shows activation

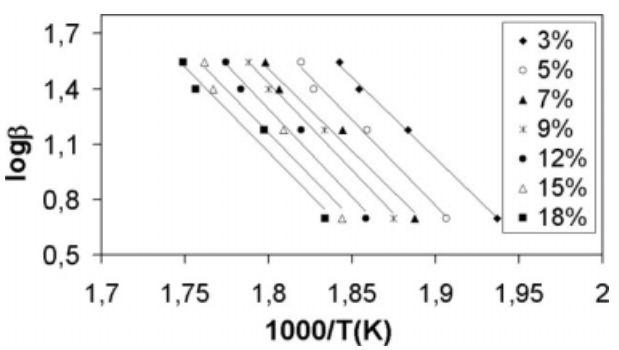

Figure 7 Flynn–Wall–Ozawa method applied to the experimental data (3–18%).

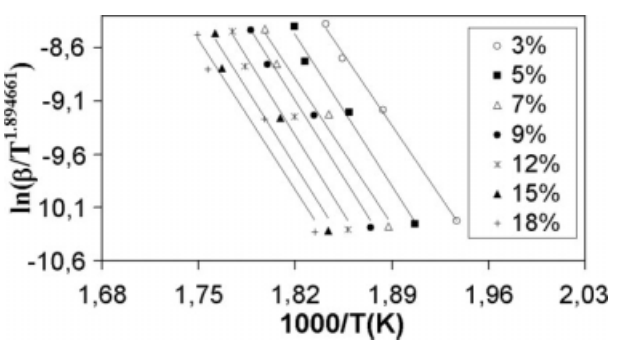

Figure 8 Tang method applied to the experimental data (3–18%).

TABLE IV
Activation Energy (E_a) Values Obtained with the Coats–Redfern Method for Several Solid-State Processes at Heating Rates of 5 and 15°C/min

	5°C/min		15°C/min	
Mechanism	E_a (kJ/mol)	R	E_a (kJ/mol)	R
A_2	68.55	0.9978	85.41	0.9997
A_3	42.76	0.9975	53.93	0.9997
A_4	29.86	0.9972	38.19	0.9997
R_1	139.24	0.9987	171.67	0.9998
R_2	142.55	0.9984	175.72	0.9998
R_3	143.67	0.9983	177.10	0.9998
D_1	287.32	0.9988	352.36	0.9998
D_2	316.62	0.9986	357.73	0.9998
D_3	296.15	0.9984	363.23	0.9998
D_4	293.18	0.9985	359.56	0.9998
F_2	4.76	0.5773	7.66	0.7374
F_3	18.35	0.8328	24.36	0.8750

energies and correlations obtained with deceleration mechanisms and the Horowitz–Metzger model, which uses ln $g(\alpha)$–$(T - T_r)$ plots with eq. (8). Again, the best agreement with the Flynn–Wall–Ozawa and Tang methods corresponded to an R_1 deceleration mechanism. In particular, the activation energy at a heating rate of 25°C/min was 167.09 kJ/mol, which was very close to the value obtained with the Tang method (167.47 kJ/mol), and the correlation (0.9822) was in good agreement with the value obtained with the Kissinger method (0.9867).

According to the Criado method,[22] the determination of the mechanism of a solid-state process may be easy and precise. This method employs reference theoretical curves called master plots, which are compared to experimental data. Experimental results were obtained from eq. (9) at a heating rate of 15°C/min, which was considered optimum from studies based on integral methods. Figure 9 shows master curve plots of $z(\alpha)$ versus α. Because we used the Doyle approximation, only conversion values in the range of 3–18% are considered for discussion in this article. The experimental results showed better agreement with the $z(R_1)$ master curve in this range of conversions, which corresponded to an R_1 deceleration mechanism, as can be seen in Figure 9.

TABLE V
Activation Energy (E_a) Values Obtained with the Coats–Redfern Method for Several Solid-State Processes at Heating Rates of 25 and 35°C/min

	25°C/min		35°C/min	
Mechanism	E_a (kJ/mol)	R	E_a (kJ/mol)	R
A_2	67.31	0.9837	78.35	0.9965
A_3	41.79	0.9812	49.15	0.9961
A_4	29.03	0.9780	34.55	0.9956
R_1	137.06	0.9836	158.38	0.9974
R_2	140.42	0.9847	162.13	0.9972
R_3	141.55	0.9851	163.39	0.9971
D_1	283.37	0.9847	326.01	0.9975
D_2	287.81	0.9854	330.96	0.9974
D_3	292.35	0.9861	336.04	0.9972
D_4	289.32	0.9856	332.65	0.9973
F_2	4.59	0.7207	6.15	0.6436
F_3	18.41	0.9100	21.56	0.8453

TABLE VI
Activation Energy (E_a) Values Obtained with the Van Krevelen Method for Phase-Boundary-Controlled Reaction Processes at Different Heating Rates

Heating rate (°C/min)		Mechanism		
		R_1	R_2	R_3
5	E_a (kJ/mol)	152.03	155.53	156.71
	R	0.9990	0.9989	0.9988
15	E_a (kJ/mol)	187.20	191.52	192.98
	R	0.9997	0.9998	0.9998
25	E_a (kJ/mol)	150.01	153.58	154.79
	R	0.9840	0.9851	0.9854
35	E_a (kJ/mol)	172.82	176.80	178.14
	R	0.9977	0.9976	0.9976

CONCLUSIONS

The copolymerization of MBMA and IBMA initiated with ethyl 2-bromoacetate was carried out by ATRP. The synthesized copolymer, poly(MBMA-*co*-IBMA), was characterized with ^{1}H-NMR, ^{13}C-NMR, FTIR, and gel permeation chromatography techniques. The copolymer composition was calculated with the aid of integration heights, and the percentages of MBMA and IBMA were determined to be 76 and 24%, respectively. The M_n and molecular weight distribution values of poly(MBMA-*co*-IBMA) were found to be 12,500 and 1.5, respectively. The copolymerization was controlled/living. The thermal degradation kinetics of the copolymer was also investigated with various methods of thermogravimetric

TABLE VII
Activation Energy (E_a) Values Obtained with the Horowitz–Metzger Method for Phase-Boundary-Controlled Reaction Processes at Different Heating Rates

Heating rate (°C/min)		Mechanism		
		R_1	R_2	R_3
5	E_a (kJ/mol)	174.86	181.74	184.89
	R	0.9991	0.9990	0.9990
15	E_a (kJ/mol)	204.39	211.94	215.31
	R	0.9995	0.9997	0.9998
25	E_a (kJ/mol)	167.09	173.93	177.08
	R	0.9822	0.9833	0.9837
35	E_a (kJ/mol)	190.47	197.74	201.04
	R	0.9978	0.9977	0.9977

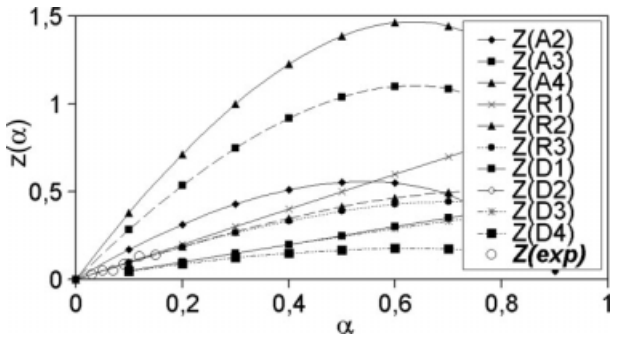

Figure 9 Master plots of theoretical $Z(\alpha)$ values and experimental $z(\alpha)$ [z(exp)] values (3–18%).

analysis. The activation energy values of poly (MBMA-*co*-IBMA) obtained with the Kissinger, Flynn–Wall–Ozawa, and Tang methods were 166.38, 167.54, and 167.47 kJ/mol, respectively. Also, we discussed the applicability of the master plots based on the first derivative of α for determining the mechanism of a solid-state process. An analysis of the experimental results suggested that the reaction mechanism was an R_1 deceleration type in the conversion range studied.

References

1. Chiefari, J.; Chong, Y. K.; Ercole, F.; Krstina, J.; Jeffery, J.; Le, T. P. T.; Mayadunne, R. T. A.; Meijs, G. F.; Moad, C. L.; Moad, G.; Rizzardo, E.; Thang, S. H. Macromolecules 1998, 31, 5559.
2. Moad, G.; Rizzardo, E.; Solomon, D. H. Macromolecules 1982, 15, 909.
3. Patten, T. E.; Xia, J. H.; Abernathy, T.; Matyjaszewski, K. Science 1996, 272, 866.
4. Wang, J. S.; Matyjaszewski, K. J Am Chem Soc 1995, 117, 5614.
5. Matyjaszewski, K.; Xia, J. H. Chem Rev 2001, 101, 2921.
6. Demirelli, K.; Kurt, A.; Coskun, M. Eur Polym J 2004, 40, 451.
7. Demirelli, K.; Coskun, M.; Kaya, E. J Polym Sci Part A: Polym Chem 2004, 42, 5964.
8. Heuts, J. P. A.; Davis, T. P. Macromol Rapid Commun 1998, 19, 371.
9. Payene, H. F. Organic Coating Technology; Wiley: New York, 1964; Vol. 1.
10. Martin, C. R. Technology of Paints, Varnishes and Lacquers; Reinhold: New York, 1968.
11. Warson, H. The Application of Synthetic Resin Emulsion; Ernest Benn: London, 1972.
12. George, D. C.; Edward, I.; Ewald, L. Eur. Pat. Appl. EP 155,231 (1985); George, D. C.; Edward, I.; Ewald, L. Chem Abstr 1986, 104, 177740H.
13. Hans, S.; Albert, E.; Peter, J. K.; Reinhold, L. J. Ger. Offen. DE 3,331,691 (1985); Hans, S.; Albert, E.; Peter, J. K.; Reinhold, L. J. Chem Abstr 1985, 103, 11348h.
14. Kuo, S. W.; Kao, H. C.; Chang, F. C. Polymer 2003, 44, 6873.
15. Wilkie, C. A. Polym Degrad Stab 1999, 66, 301.
16. Jellinek, H. H. G.; Luh, M. D. J Phys Chem 1966, 70, 3672.
17. Dogan, F.; Akat, H.; Balcan, M.; Kaya, I.; Yurekli, M. J Appl Polym Sci 2008, 108, 2328.
18. Núnez, L.; Fraga, F.; Fraga, L.; Rodriguez, J. A. J Therm Anal 1996, 47, 743.
19. Nunez, L.; Fraga, F.; Nunez, M. R.; Villanueva, M. Polymer 2000, 41, 4635.
20. Flynn, J. H. J Therm Anal 1988, 34, 367.
21. Hatakeyama, T.; Quinn, F. X. Thermal Analysis: Fundamentals and Applications to Polymer Science; Wiley: Chichester, England, 1994.
22. Criado, J. M.; Málek, J.; Ortega, A. Thermochim Acta 1989, 147, 377.
23. Ma, S.; Hill, J. O.; Heng, S. J Therm Anal 1991, 37, 1161.
24. Kissinger, H. E. Anal Chem 1957, 29, 1702.
25. Flynn, J. H.; Wall, L. A. J Res Natl Bur Stand Sect A 1966, 70, 487.
26. Ozawa, T. Bull Chem Soc Jpn 1965, 38, 1881.
27. Doyle, C. D. Nature 1965, 207, 240.
28. Tang, W.; Liu, Y.; Zhang, C. H.; Wang, C. Thermochim Acta 2003, 40, 839.
29. Coats, A. W.; Redfern, J. P. Nature 1965, 207, 290.
30. Van Krevelen, D. W.; Van Heerden, C.; Huntjons, F. J. Fuel 1951, 30, 253.
31. Horowitz, H. H.; Metzger, G. Anal Chem 1963, 35, 1464.
32. Senum, G. I.; Yang, K. T. J Therm Anal 1977, 11, 445.
33. Jimenez, A.; Berenguer, V.; López, J.; Sanchez, A. J Appl Polym Sci 1993, 50, 1565.